Optical, Catalytic and Electrokinetic Properties of Silver Nanoparticles of Different Sizes

A

Thesis submitted

in partial fulfillment of the requirement for the degree of

Master of Science

in

Chemistry

Under the supervision of

Dr. Bonamali Pal

Associate Professor

Submitted by:

Sonia

Registration no. 301002018

School of Chemistry and Biochemistry

Thapar University

Patiala-147004

Punjab

July 2012

Acknowledgement

I would like to convey my sincere gratitude to my research guide Dr. Bonamali Pal, Associate Professor, School of Chemistry and Biochemistry for his guidance and suggestions which helped me immensely during this course. I am extremely obliged to him for giving me such an innovative and current research topic.

I acknowledge Dr. B. K. Chudasama and Ms. Chandani, School of Physics and Material Science, Thapar University for measuring Zeta potential and DLS particle size distribution.

I express my sincere thanks to Ms. Rupinder Kaur and Anila (Ph.D Scholars) for their timely help and constant support throughout my project.

I am highly indebted to my loving parents for their inspirations, blessings, and financial support.

God's grace has kept me on the path of success and helped me in completion of this project.

Sonia

Sonia

Date:

Place: Thapar University,
Patiala (Punjab).

Candidate's Declaration

I hereby declare that the work being presented in the thesis entitled **"Optical, Catalytic and Electrokinetic Properties of Silver Nanoparticles of Different Sizes"** in partial fulfillment of the requirement for the award of the degree of Master in Chemistry, School of Chemistry and Biochemistry, Thapar University, Patiala, is my own work during the period of Jan 2012 to May 2012, under the supervision of Dr. Bonamali Pal, Associate Professor, School of Chemistry and Biochemistry, Thapar University, Patiala. I have not submitted the matter embodied in this thesis for the award of any other degree.

Patiala

Sonia Sonia

Date:

Registration no. 301002018

This is to certify that the above statement made by the candidate is correct and true to the best of our knowledge.

Dr. Bonamali Pal

Associate Professor

School of Chemistry & Biochemistry,

Thapar University, Patiala

Dr. Satnam Singh

Professor & Head

School of Chemistry & Biochemistry,

Thapar University, Patiala

Certificate

This is to certify that the thesis entitled **"Optical, Electrokinetic and Catalytic Properties of Synthesized Silver Nanoparticles with Different Sizes"** being submitted by Ms. Sonia in partial fulfillment of the requirement for the award of degree of Master of Science in the School of Chemistry and Biochemistry, Thapar University, Patiala, is carried out under the supervision of Dr. Bonamali Pal and that no part of this thesis has been submitted for the award of any other degree.

Dr. Bonamali Pal

Associate Professor

School of Chemistry & Biochemistry,

Thapar University, Patiala

Dr. Satnam Singh

Professor & Head

School of Chemistry & Biochemistry,

Thapar University, Patiala

Dr. S.K Mohapatra

Dean, Academic Affairs

Thapar University, Patiala

LIST OF CONTENTS

Abstract

Silver nanospheres (AgNS) of five different sizes in the range between 10 to 80 nm have been prepared by reduction with sodium borohydride ($NaBH_4$) and sodium citrate ($C_6H_5O_7Na_3$) and by solvothermal process using Polyvinylpyrrolidone (PVP) and dimethylformamide (DMF). These AgNS were characterized by UV-Visible absorption spectra, transmission electron microscopy, Zeta potential (ζ) and diffuse light scattering measurements and studied their comparative catalytic properties. The AgNS prepared by utilizing PVP and DMF are found to be much larger in size ca. ≈ 30-80 nm having red shifted surface plasmon band at 474.6 nm as compared to relatively smaller AgNS sizes ca. ≈13.5 nm (SP band ≈ 392.6 nm) as obtained by reduction with $NaBH_4$ and $C_6H_5O_7Na_3$. The effects of silica (SiO_2) and PVP coating and the influences of various solvents on the optical absorption, ζ, conductance and catalytic activity of these AgNS were studied comparatively. The aqueous suspension of SiO_2 coated AgNS (SiO_2/AgNS) displayed highest zeta potential (-24.6 mV) and conductance (1927 μS) values as compared to the bare AgNS (-5.59 mV and 86 μS) in water dispersion. The catalytic activity of various AgNS depending on its size and coating agents (silica and PVP) is evaluated and compared by the reduction of *p*-nitrophenol to *p*-aminophenol. A significant increase (17.5 % to 55 %) in the catalytic activity has been found with decreasing the size (80 nm to 13.5 nm) of AgNS. An optimum amount (10.92×10^{18} atoms) of AgNS is the prerequisite for the reaction to be carried out at a higher pace (with in 36 min).

1. Introduction

Transition metals such as Au, Ag, Cu, Pt, Pd, Rh, Fe, Co, Ni, V etc. has been considered as subject of interest for many years due to their potential applications in different areas such as heterogeneous catalysis, medicinal industry, photonics, electromagnetism etc [1-4]. These metals have incomplete *d* or *f* shells in the neutral or cationic states and are used in the synthesis of many molecular complexes, organometallic compounds, and solid-state compounds such as oxides, sulfides, and halides etc [5-7]. The Iron Triad i.e. Fe, Co, Ni metals have very important applications in the industry. For example, Ni used for hydrogenation of unsaturated organics, Fe and Mo for the manufacture of NH_3 (Haber process) etc [8, 9]. Platinum group elements (Pt, Pd, Rh) form metal ligand complexes which are used for synthesis of many organic, inorganic and bioinorganic complexes [10, 11]. The most important group i.e., coinage metals (Au, Ag and Cu) are used for manufacturing the ornaments, coins, utensils from the ancient times.

But with the advent of nanoscience, the importance of metal colloids has been increased because of the effective utilization of the atoms in a particle that result in their higher productivity rate [12-14]. Nanoscience deals with the particles ranging from 1-100 nm and properties of such small metal particles changes as size of the particle approaches to nanoscale. It was demonstrated by the physicists that nanoparticles (NPs) in the diameter range 1-10 nm (intermediate between the size of small molecules and that of bulk metal) displayed electronic structures owing to quantum- mechanical rules [15]. The quantum sized particles possess unique optical, electronic, chemical, and magnetic characteristics neither those of bulk metal nor those of molecular compounds [16-18]. There are three major factors that are responsible for these differences: high surface-to-volume ratio, quantum size effect, and electrodynamic interactions [14, 18-20]. These quantum sized particles show more reactivity than bulk materials as the percentage of atoms on the surface of such material become much significant in relation to the number of atoms in the bulk of material [13, 18]. Generally, bulk atom in the interior of particles does not take part in catalytic recations. Hence, increasing surface atom of smaller particles has lead to effective utilization of important chemicals. Gold is one of the most stable noble metal in its bulk state among group-VIII elements. Because of its inertness, Au was formerly not known as a catalyst and was used in manufacturing of ornaments, utensils etc during the ancient times. But with the outcome of nanoscience, miracle happened and Haruta et al. [21, 22] demonstrated for the first time that metal oxide-

supported Au catalysts of size 2-5 nm showed unusually high catalytic activities as compared to the bulk. Significant progress has been achieved in the preparation techniques of various shapes and sizes of Au NPs and one can easily tailor the properties of noble-metal nanostructures by altering their morphology, thus improve their performance in a variety of applications such as catalysts for a variety of thermal and photoreactions [14, 23].

The high surface area to volume ratio of NPs provides unexpected optical properties as NPs are small enough to confine their electrons and produce quantum effects. Colloidal solutions of the noble metals, (namely copper, silver, and gold) have been found to exhibit characteristic colors that have received considerable attention [14, 18]. For example, gold NPs appear deep red to purple in solution. These different colors appear due to the coherent oscillation of the conduction band electrons which are induced due to interaction of electromagnetic field. When the incident photon frequency is resonant with the collective oscillation of the conduction band electrons an absorption band results and is known as the surface Plasmon resonance (SPR) [14, 18, 24-26]. SPR band is the characteristic feature of the coinage metal (Au, Ag and Cu) NPs.

The coinage metals (Cu, Ag, and Au) are exceptional because (i) they are noble and form air-stable colloids (ii) due to d-d band transitions, the Plasma frequency lies in the visible part of the spectrum and the fundamental absorption SP band of Au, Ag and Cu NPs appear at 520 nm, 420 nm and 570 nm, respectively [24-26]. The resonance frequency of this SPR is strongly dependent on particle size, shape, interparticle interactions, dielectric properties, and local environment of the colloidal solution. As the shape or size of the NPs changes, the surface geometry changes, causing a shift in the electric field density on the surface. This causes a change in the oscillation frequency of the electrons, generating different cross-sections for the optical properties including absorption and scattering. For nanorods [27], the SP resonance splits into two bands: parallel (longitudinal) and perpendicular (transverse) to the axis of the nanorods.

The unique structural and tunable optical properties of metal NPs have made them ideal materials for a wide range of biological applications such as cell labeling, imaging, gene delivering, heating, sensing and optoelectronic devices [28-33]. AuNPs shows many applications as sensors and have been used to manipulate the selectivity between solutes in capillary electrophoresis. A large range of chemical reactions are now known to be

catalysed by gold catalysts including selective oxidation and reduction of nitrogen oxides [30].

Nowadays AgNPs have attracted much attention and have found applications in diverse areas, including medicine, catalysis, textile engineering, bio-technology and bioengineering, water treatment, electronics, and optics [31-33]. Currently silver NPs are widely used as antibacterial/antifungal agents in a diverse range of consumer products: air sanitizer sprays, detergents, soaps, shampoos, toothpastes, air filters, coatings of refrigerators, vacuum cleaners, food storage containers etc. Silver NPs are considered as better catalyst than gold as Ag is cheaper than gold and the work function of silver (4.26 eV) is much lower than that of gold (5.1 eV) and copper (4.65 eV), that is responsible for better electron transfer rate [34].

Although study of silver nanostructures has made great progress, still there are very few papers reporting catalytic activity of silver NPs of different shapes and sizes [35]. The main drawback of using AgNPs as catalyst is that these are highly prone to oxidize, form silver oxide and hence, do not show true catalytic activity. Therefore, we need some surface protecting agent such as glutathiol, disulfides, alkyl thiols, mercapto silane, xanthates and amino acids to stabilize the NPs [36-39]. But due to the presence of these capping agents on the nanoparticle surface, optical and catalytic properties are blocked to a certain extent because being chemical in nature, these surface agents itself start to reduce or oxidise. Therefore we need such an inert protecting group that would not interfere in the reaction kinetics. For example, the optical properties of silica-coated gold NPs were easily tuned depending on the thickness of silica shell and it will prevent the aggregation of NPs [38].

The functionality and stability of a NP also show alteration depending on its surface charge that was influenced by the environmental ionic conditions, pH of the medium polarity of solvents and surface coating agents [40]. In this context, Liao et al. [41] observed the chain like aggregation of gold nanospheres (AuNS) on changing the surrounding medium (water to ethanol) and found that dipole-dipole interaction and asymmetric distribution of the charges were responsible for such aggregation of AuNPs. There is no such report is available for the silver NPs and hence, it needs some exploration. So, it is valuable to investigate the effect of shape, size with polarity of solvents and surface charge of various nanostructures that would further affect the optical and catalytic properties.

Therefore, here we synthesized Ag nanospheres (AgNS) of various sizes (10 to 80 nm) employing sodium citrate and sodium borohydride as a reducing agent and to prevent them from oxidation, silica and PVP coating was done. Furthermore, optical absorption spectra, and zeta potential (ζ) measurements were examined for the various sizes of AgNS. Silver NPs have been used to catalyze the reduction of *p*-nitrophenol to *p*-aminophenol as a model compound. It has been chosen because *p*-aminophenol is a commercially important chemical intermediate used in the manufacture of several analgesic and antipyretic such as paracetamol, acetanilide, and phenacetin etc [42]. Apart from pharmaceuticals, p-aminophenol is also used in manufacturing various industrial dyes such as sulfur and azo dyes, which are especially useful in dying hair, furs and feathers.

2. Literature survey

Many methods for the synthesis of AgNPs of different shapes and sizes and their optical properties have been reported in the literature. Filippo et al. [43] reported the synthesis of different silver nanostructures (including nanospheres, neckles and nanowires) synthesized from a solution of $AgNO_3$ and β-D glucose under microwave irradiation without using any reducing or capping agent. It was observed that SPR band for spherical AgNPs was found to be at 410 nm having size range 12 ± 6 nm that was confirmed by TEM images. Nam et al. [44] demonstrated the preparation of AgNPs by using $AgNO_3$ in aqueous solution of poly(ethylene glycol) (PEG), which acted as reducing and stabilizing agent. Silver NPs (3.68 ± 1.03 nm) were produced by the entangled PEG 100, but very low concentrations of silver NPs were obtained by the single-coiled PEG 2 and PEG 35. Bogle et al. [45] represented the synthesis of AgNPs by irradiating (with 6 MeV electrons) the mixture of $AgNO_3$ and poly-vinyl alcohol (PVA) and was characterized by UV-Vis spectroscopy, SEM, TEM and XRD techniques. Absorbance peak at 455 nm gave the evidence for the formation of AgNPs and TEM analysis depicts their spherical and cubic shape.

However, AgNPs are very sensitive to air and oxidised easily, so it is very important to coat the particles to utilize them effectively. In this context, a number of reports have been cited and it is gaining interest nowadays to overcome the difficulties related with uncoated NPs like non-desired aggregation processes, low stability and high chemical reactivity. Various methods are employed for coating the particles such as Stober method, use of silane coupling agents, and the sodium silicate water-glass method etc. Sarkar et al. [46] discussed the synthesis of AgNPs by reducing the Ag ions with NaOH in ethylene

glycol and glycerol without adding any external reducing agent. The formed NPs were stabilized by PVP or sodium dodecylsulphate and the particles stabilize by PVP show absorbance band at 415 nm having size range 25 ± 2 nm. It is also mentioned that PVP and silica stabilized particles remains stable for one year, whereas SDS stabilized particles do not show such stability. Similarly Patel et al. [47] also used the PVP as a stabilizing agent for the preparation of AgNPs by microwave technique. Santos et al. [48] reduced the silver salt with DMF in presence of PVP to form the AgNPs of different shape and sizes, by using both microwave and reflux method. Kobayashi et al. [49] reported the silica coating of AgNPs by stober method using dimethylamine (DMA) as a catalyst.

The stability of NPs can also be controlled by Zeta potential/surface charge/surrounding medium which are important parameters to study for making stable colloidal solution. Surface charge of the NPs was modified on coating them with different substrates, by changing their surrounding medium, pH and ionic strength of the solution. For example, Badawy et al. [39] investigated the stability of four different type of AgNPs i.e. (a) uncoated AgNPs (H_2-AgNPs), (b) electrostatically stabilized (citrate and $NaBH_4$-AgNPs), (c) sterically stabilized (polyvinylpyrrolidone (PVP)-AgNPs) and (d) electrosterically stabilized (branched polyethyleneimine (BPEI)-AgNPs) and their zeta potential values are -22 mV, -40 mV, -3 mV, and +8.9 mV, respectively. It has been shown that H_2-AgNPs, citrate, and $NaBH_4$-coated AgNPs are aggregated at higher ionic strengths (100 mM, $NaNO_3$) and acidic pH (3.0) but PVP coated AgNPs do not show any such aggregation effects.

Extensive study of catalytic activity has also been done with AuNPs and it was found that the catalytic activity of AuNPs depends on its shape, size, oxidation state, surface support and electronic and chemical properties of the material. In this regard, various shapes and sizes Au nanostructures (including nanocages, boxes, cubes, spheres, wires etc.) has been used as a catalyst to carry out the nitro-aromatic reduction [42, 50]. In this view, Chirea et al. [51] described the chemical reduction of *p*-nitroaniline to diaminophenylene using gold nanowires as catalyst and the obtained result suggests that the reaction was six times faster in presence of gold nanowires. However, there are very few reports are available in the literature about catalytic activity and electrokinetic studies of AgNPs. AgNPs act as good antimicrobial agents and can be used as effective growth inhibitors in various microorganisms, in medical devices, antimicrobial control systems. Kim et al. [52] reported the antimicrobial activity of AgNPs against yeast, *Escherichia coli*, and *Staphylococcus aureus*.

AgNPs show photocatalytic activity and are useful to promote light induced electron-transfer reactions. Hirakawa et al. [53] demonstrated the photoinduced charging and dark discharging of electrons in a silver core-semiconductor shell structure. The high activity and selectivity in the Ag/TiO_2-photo catalyzed reduction was rationalized in terms of the charge separation efficiency, the selective adsorption of the reactants on the catalyst surfaces, and the restriction of the product desorption [54].

3. Research gap

From the literature survey, it is revealed that extensive work has been done on the synthesis and characterization of different shapes and sizes of AgNPs till now. But little work has been done to correlate the catalytic activity of different sizes of AgNS. Catalytic property of a metal NP is mainly determined by its size, shape, composition, crystallinity, and structure. Due to different sizes, their geometric surface area, surface to volume ratio and number of surface exposed atoms vary and hence, the rate of reaction. There are very few studies in which catalysis is conducted with AgNS of different sizes in colloidal solution. Industrial implementation of AgNS as a catalyst would have much viable practical value and provides a better cost effective tool over the use of costly metal NPs (Au, Pt, Pd and Rh).

As AgNS easily undergoes oxidation in arid atmosphere and to prevent them from oxidation, different capping agents such as alkyl thiols, mercaptosilane and PVP has been employed. These capping agents being chemically reactive in nature hinder the reaction and itself get oxidized or reduced in the reaction media. Therefore, we require such an inert coating agent that will not hamper the reaction rate and as a result the true catalytic activity of NP can be judged. Hence, silica being protective, porous, transparent, and inert agent would not affect the rate of reaction and also prevent the aggregation of particles.

Moreover, no report has been found that showed the effect of changing the surrounding medium on the optical property of AgNS but account on the alteration of absorption features and size of the AuNPs is available [41].

Furthermore, functionality of a NP is determined by its surface charge, zeta potential and conductivity and was influenced by the pH and dipole moment of the dispersion medium. The surface charge governs the stability of colloidal particles and the influence of particle size for displaying highest optical and catalytic properties that could be actually defined on the basis of quantum size effect. But, there are rare reports on the zeta potential

and surface charge of AgNS dependent on their size in any solvent (polar and non-polar) is available in the literature. So keeping this research gap in view, following objectives are defined.

4. Objectives:

1. Synthesis of various sizes of Ag nanospheres using sodium citrate, sodium borohydride and PVP as a reducing agent.
2. Synthesis of silica and PVP coated nanospheres to prevent them from oxidation and to compare their catalytic activity with uncoated nanospheres.
3. Investigation of characteristic absorption band of various sizes of AgNS by UV-Vis spectrophotometer and TEM size and shape analysis. Measurement of zeta potential (ξ) and DLS particle size distribution of AgNS in different polar and non-polar solvents.
4. Study of catalytic activity of AgNS for *p*-nitrophenol reduction to aminophenol as a model reaction because aminophenol is an important intermediate for medicines, dyes and organic synthesis.

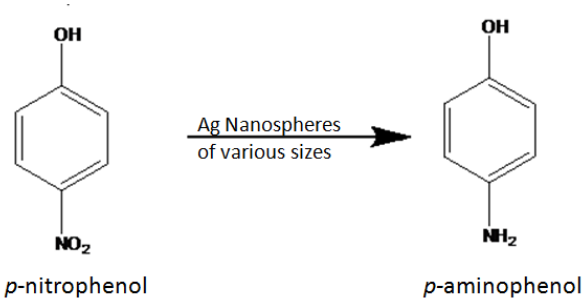

p-nitrophenol *p*-aminophenol

5. Experimental Section

(i) Material and methods

Materials used: Silver nitrate **(**$AgNO_3$) was purchased from Fisher Scientific, sodium borohydride ($NaBH_4$) was purchased from RANKEM, trisodium citrate ($C_6H_5O_7Na_3$) was purchased from SDFCL. DMF (dimethylformamide), PVP (Polyvinylpyrrolidone), ammonia, and ethanol were used as received from Loba chemie, India. TEOS (tetraethyl-orthosilicate) was purchased from Merck. Deionized water was obtained using an ultrafiltration system (Milli-*Q*, Millipore) with a measured conductivity above 35 mho cm^{-1} at 25 °C.

(ii) Synthesis of silver nanospheres of different sizes

The Ag nanospheres were synthesized by mixing 2 ml $AgNO_3$ (1 mM) and 6 ml $NaBH_4$ (2 mM) with constant stirring for about an hour until a greenish colour was obtained by keeping the whole reaction at 0˚C. These as synthesized AgNS having size range of 13.5 nm and were so stable that did not change colour for several months without any stabilizing agent [52].

AgNS of ≈ 22 nm were prepared by employing trisodium citrate as a reducing agent and was added dropwise (3 ml, 1% trisodium citrate) in the boiling aqueous solution of $AgNO_3$ (0.001 M, 30 ml) under constant stirring until the colour changes from pale yellow to green. Then solution was removed from the heating element and cooled to room temperature [55].

(iii) Silica coating of silver nanospheres

The citrate reduced nanospheres (5 ml, 2.73×10^{21} atoms) was taken in a round bottom flask and ammonia (100 µl) was added to it followed by the addition of 100 µl ethanolic solution of TEOS (557.9 µl TEOS in 9.4 ml ethanol, 0.25 M). Then solution was refluxed for 18 h. After that it was centrifuged to remove the excess ethanol from the solution [49].

(iv) Synthesis of PVP coated silver nanospheres

Silver NPs of different sizes were synthesized by employing one-step seedless solvothermal reduction route as reported. The AgNS were prepared by dissolving of $AgNO_3$ (689.67 mg, 203 mM) and PVP (93.24 mg, 42 mM) in DMF (20 ml) contained in round bottom flask and reaction mixture was stirred for 10 min at room temperature. Then refluxing of the above solution was done at 120˚C for different times i.e. 2h, 4h and 6h to obtain nanospheres of three different sizes, respectively. The samples were cooled at room temperature and washed with water to separate from DMF and PVP during centrifugation for four to five times and finally, NS were dispersed in 20 ml deionized water [56, 57].

(v) Dispersion of Ag Nanospheres in different solvents

AgNS of different sizes were dispersed in various polar (ethanol, and DMSO) and non polar solvents (heptane) to examine their optical property, Zeta potential and DLS (Diffuse Light Scaterring). The aqueous solution of AgNS (20 µl, no. of Ag atoms = 10.9×10^{18}

atoms) were dispersed in 20 μl of solvent (ethanol, DMSO, heptane) and then diluted upto 3 ml. This solution was further diluted by taking 13 μl (4.7×10^{16} atoms) of it in 1.5 ml water and examined for SPR and electrokinetic studies. In case of PVP coated AgNS, 60 μl (4.76×10^{16} atoms) of AgNS was diluted in 1.5 ml of water and was used for the SPR, DLS and electrokinetic studies. The size of AgNS was analysed by TEM (Hitachi 7500, 2Å, 120 KV), Zeta potential determination was conducted by (Brook heaven 7610).

(vi) Catalytic activity

Catalytic activity of synthesized AgNS was examined by reducing *p*-nitrophenol (PNP) using $NaBH_4$ as a reducing agent. The catalytic reduction of *p*-nitrophenol was carried out by adding 500 μl of ice-cold $NaBH_4$ solution (0.42 M) to 5 ml of PNP (0.09 mM), and the solution was vigorously stirred for 5 min at room temperature. After that, the calculated amount (5.4×10^{18} atoms) of the AgNS of various sizes was added to initiate the reduction reaction of PNP to *p*-aminophenol (PAP) and was monitored by measuring the absorption spectra (PNP, $\lambda_{max} \approx 400$ nm and PAP, $\lambda_{max} \approx 300$ nm) at regular time intervals.

(Vii) Characterization:

Optical properties were analyzed by UV-Vis absorption (Specord 205) spectrophotometer and spectrofluorimeter (Perkin-Elmer LS55). Transmission electron microscope (TEM) photographs were taken on Hitachi 7500 model with resolution 2A° operating at voltage 120 kV. The reduction of *p*-nitrophenol to its main reduction product, *p*-aminophenol, was monitored using UV-Vis spectrophotometer. Zeta potential and diffuse light scattering (DLS) measurement was conducted using Brook heaven 7610.

5. Results and discussion

Before discussing the section 5, the various synthetic techniques for the preparation of AgNS have summarized in Table.1.

Table. 1 Tabular representation of the various experimental conditions for the synthesis of five different types of AgNS

Sample Code	$AgNO_3$ Used (mg)	Reducing Agent (mg)	Reducing*/Refluxing** Time (min)	Refluxing Temperature (°C)
AgNS-1	339	Sodium borohydride (0.45)	1-2*	100
AgNS-2	5.09	Sodium Citrate (30)	35*	0
AgNS-3	689.67	PVP (93.3)	120**	120
AgNS-4	689.67	PVP (93.3)	240**	120
AgNS-5	689.67	PVP (93.3)	360**	120

(i) Optical properties of Ag nanospheres of various sizes

The surface Plasmon resonance band (SPR band) of aqueous colloidal solution of AgNPs as a function of their particle size is shown in figure 1. The light green colour particles of

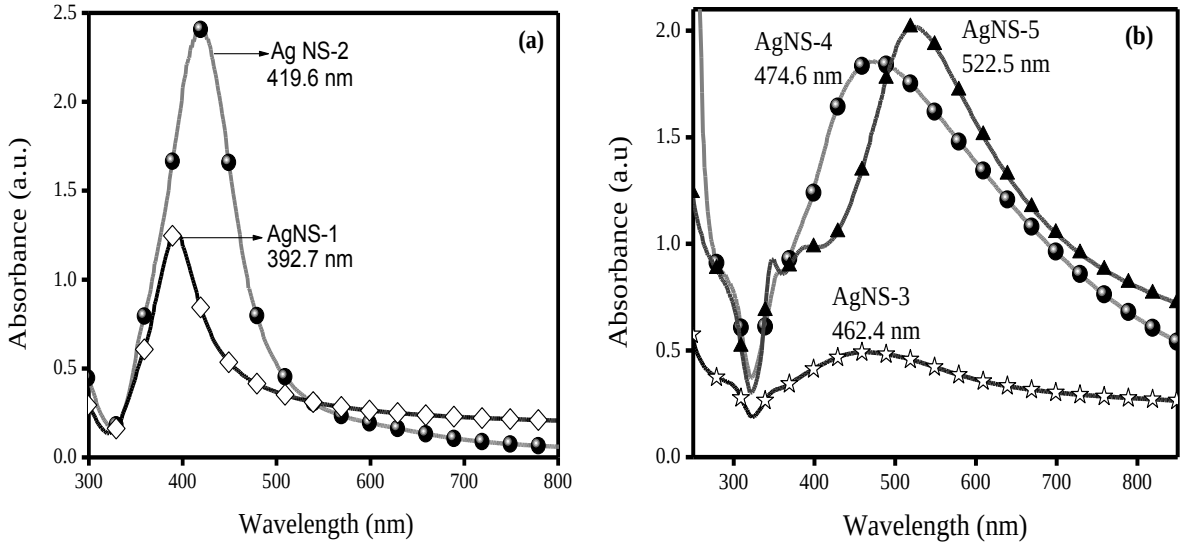

Figure. 1 Optical absorption spectra of different sizes of AgNS (a) AgNS-1 and AgNS-2 (b) AgNS-3 AgNS-4 and AgNS-5.

AgNS-1

displayed their SPR band at 392.7 nm that corresponds to their spherical shape with average size of 13.5 nm (fig.1a) [52]. Similar result was reported by Kim et al. that involve the reduction of $AgNO_3$ by $NaBH_4$ for the synthesis of AgNS displaying SP band at 390 nm with size ≈ 13.4 nm [52]. The SPR band at 419.6 nm of AgNS-2 represents the spherical shape of NPs and are larger in size as compared to the AgNS-2 (SPR band = 392.6 nm) as red shift in the SPR band (392.6 nm to 419.6 nm) depicts the enhancement in the size of NS. Ratyakshi et al. [55] observed the SPR band at 420 nm by employing $C_6H_5O_7Na_3$ as a reducing agent and resulted in the formation of 10-20 nm sized NS [27].

Fig. 1b shows the SPR band at 462.4 nm, 474.6 nm and 522.5 nm corresponding to PVP coated AgNS (AgNS-3, AgNS-4, AgNS-5) with three different sizes of ≈ 41.6 nm, ≈ 50 nm, ≈ 80 nm, respectively [56,57]. Silvert et al. obtained the similar result by utilizing $AgNO_3$ and PVP in DMF and found that PVP act as a weak reducing agent to reduce the Ag^+ to small AgNPs, which further act as seeds for the growth of large sized NPs. Moreover, when the reaction mixture was heated at 120 °C for longer time periods (upto 6h), the small NPs progressively disappeared and merge to form the larger ones through Ostwald ripening process [56].

The sharp and highly intense SP band of AgNS-2 (fig. 1a) represents the homogeneity and monodispersity of the NS as compared to the broadened, red shifted and less intense SP bands for AgNS-3, AgNS-4 and AgNS-5 in Fig 1b. This red shifting and broadening of the SP band in Fig 1b (PVP coated particles) reveal that there must be a change in the particle size distribution and surface morphology of AgNS that causes light scattering and Plasmon oscillation and hence, increasing the Plasmon linewidth [58]. It has been reported that with the increase in the particle size, SPR band continues to show red shift and becomes broadened [26].

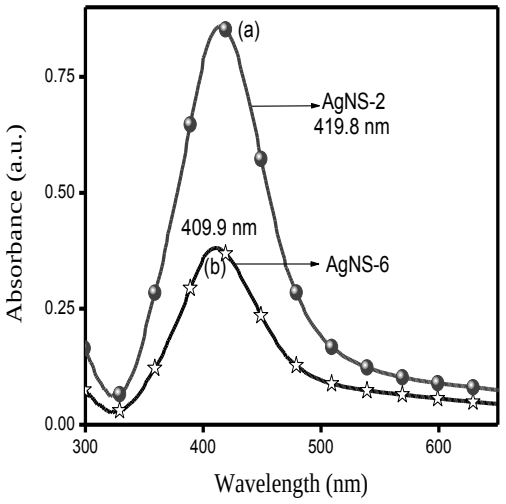

Figure. 2 SPR band of (a) AgNS-2 and (b) silica coated AgNS-6.

The use of PVP as a protective, reducing, as well as stabilising agent have some disadvantages too as it sticks on the particle surface, causes broadening in the SP band and hamper the rate of reaction. So, to overcome all these hindrances, such an inert coating material is needed that would perform a dual role, i.e. neither allow the particles to aggregate nor hinder the rate of reaction. Hence, silica being chemically inert, porous and optically transparent does not affect redox reactions at the core surface and can be easily monitored spectroscopically. Therefore, AgNS-2 was coated with silica to prevent oxidation and coagulation.

Fig. 2 shows the comparative optical absorption spectra of bare (AgNS-2) and silica coated (AgNS-6) AgNS. Silica coating was done by adding ammonia (100 µl) and ethanolic solution of TEOS (0.25 M) to AgNS-2 (5 ml) followed by stirring for 18 h. The decrease in the intensity of the absorption band has been seen along with the blue shift at 409.9 nm as compared to the bare AgNS-2 (SP band ≈ 419.6 nm). Kobayashi et al. found that scattering of light from silica shell changes the refractive index is the reasons for blue shift in the SPR band. The lowering of SPR band intensity indicates that silica shell promotes the scattering at lower wavelength [49]. The thickness of silica shell can be controlled by varying the molar ratio of TEOS to AgNS that will be helpful in studying the progression of some new optical and catalytic properties.

(ii) Size and shape analysis by TEM and DLS study

The TEM images in figure 3 reveal that the average size of the monodisperse AgNS-1 (formed by $NaBH_4$) is ≈ 13-15 nm that corresponds to sharp and intense SP band at 392.7 nm. Kim et al. [52] reported the similar result for AgNS displaying SP band at 391 nm corresponding to the particles size 13.4 nm.

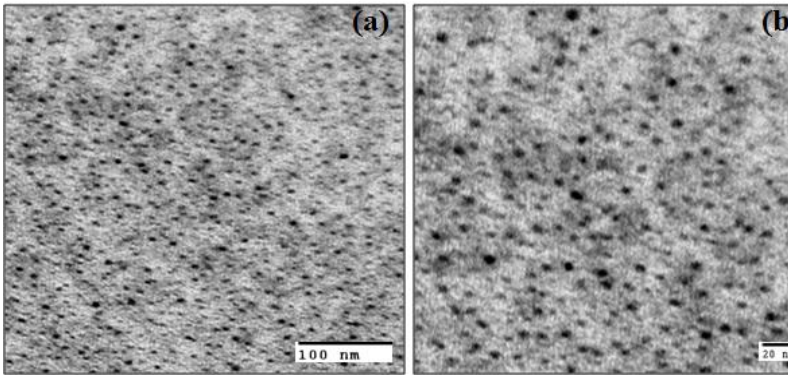

Figure. 3 TEM images of AgNS-1 formed by $NaBH_4$ reduction.

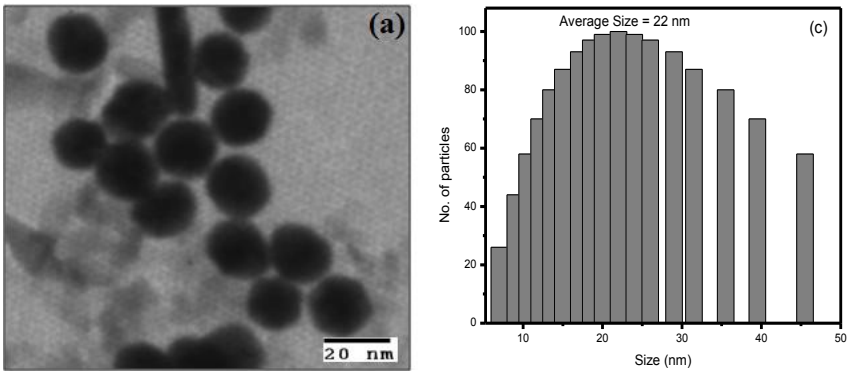

Figure. 4 (a) TEM images of AgNS-2 (SPR band = 419.6 nm, size ≈ 22 nm) formed by Na-citrate as reducing agent) and (b) size distribution of AgNS-2 in water (size range ≈ 10-45 nm).

Fig. 4a displayed the TEM image of AgNS-2 (Na-citrate as reducing agent) and having SP band at 419.6 nm corresponds to size range ≈ 22 nm. In order to further confirm the size of AgNS-2 by diffuse light scattering (DLS) measurement was analysed. The size distribution of AgNS-2 in aqueous suspension was found to be in the range of 10-45 nm with average size ~ 22 nm as shown in fig. 4b.

The AgNS-3 particles (formed by refluxing $AgNO_3$, PVP and DMF) for 4 h at 120˚C) shows larger anisotropic particles formation as shown in Figure 5. Particles synthesized by using PVP are not perfectly spherical and found to be larger in size in

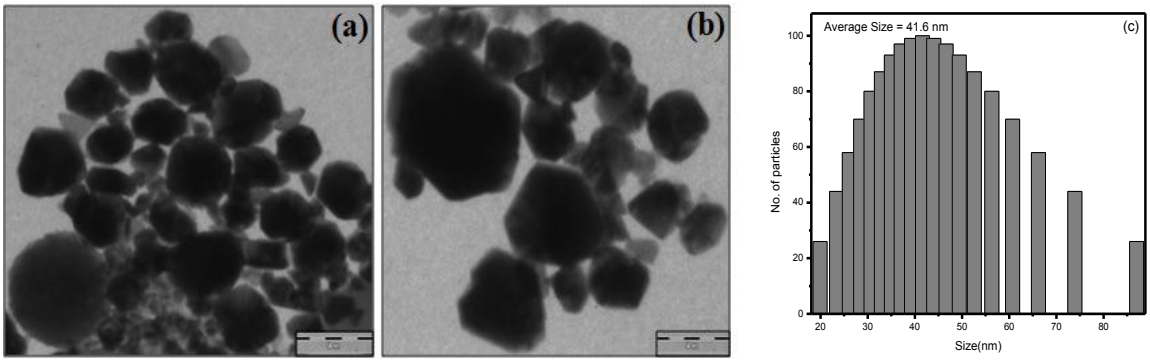

Figure. 5. TEM images of AgNS-3 (SPR band = 474.6 nm, average size ≈ 41.6 nm) formed by refluxing the reaction mixture ($AgNO_3$ + PVP +DMF) for 4 h and (c) size distribution of AgNS-4 in water (size range ≈ 20-80 nm).

comparison to AgNS-1 and AgNS-2 (fig.3 and 4). Since, PVP is a homopolymer whose individual unit contains an imide group in which N and O atoms of this polar group have a strong affinity for silver ions and metallic silver. Therefore, PVP macromolecule in solution adopts a pseudo-random coil conformation that takes part in some form of association with the metal atoms and thus increasing the probability of large sized particle formation [56, 57]. The AgNPs seen in the fig. 5a are irregular in shape and was found to be in the range of 35-50 nm with their average size ≈ 41.6 nm as found from TEM image and DLS (fig. 5c) size distribution.

(iii) Effect of solvent polarity on the optical property

Figure 6a and b showed the effect of different solvents (water, ethanol, DMSO and heptane with dipole moment = 1.85 D, 1.68 D, 3.96 D and 0 D, respectively) dispersion of AgNS on the SPR band of AgNS-2 and AgNS-4, respectively. It has been reported by J. Liao et al. [41] that ethanol addition to AuNS resulted red shift in the characteristic SPR band (520 nm to 557 nm) along with the appearance of new absorption band at longer wavelength (> 970 nm) that corresponds to aggregation. But, there is no such change in the absorption band of AgNS-2 and AgNS-4 has been observed on the dispersing the NS in the solvents of varying polarity.

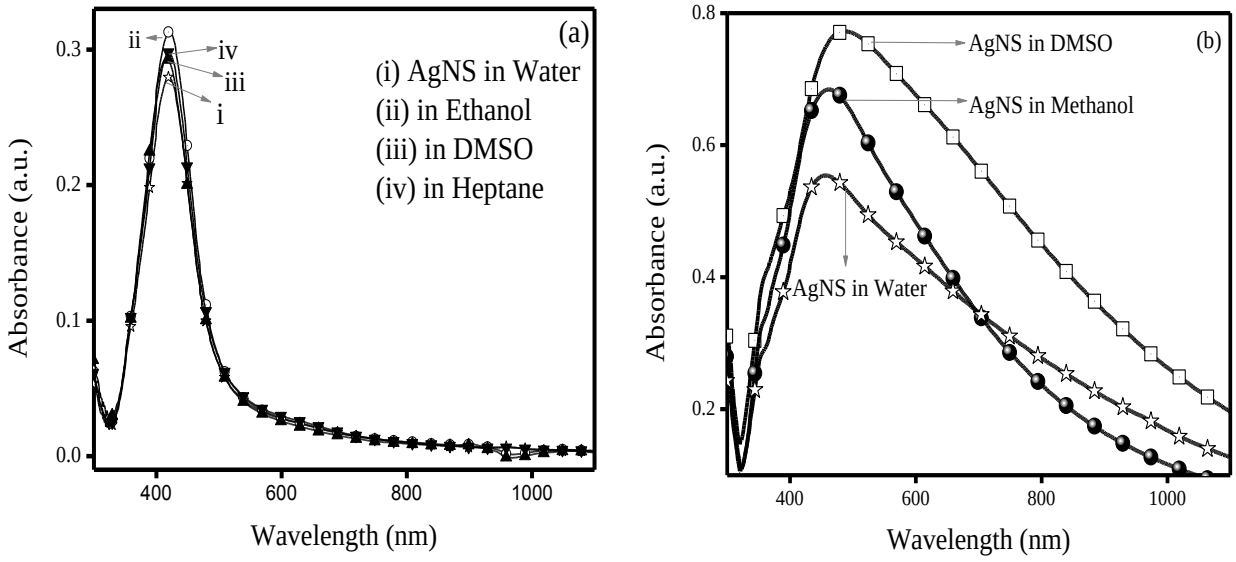

Figure. 6 Effect of addition of various polar and non-polar solvents on the surface Plasmon resonance band of (a) AgNS-2 and (b) AgNS-3.

Fig. 6a displaying the absorption spectra for AgNS-2 (prepared by using sodium citrate as reducing agent) dispersed in various polar (ethanol and DMSO) and non-polar (heptane) Solvents. There is no significant change in the SPR band of AgNS-2 has been observed as these were electrostatically stabilized by the adsorption of the negatively charged citrate ions on their surface [55]. Therefore, the interaction among the AgNS and surrounding medium has been prevented thereby, resulted in the sharp and intense SP band that describes its non-aggregation behaviour. Similarly, fig. 6b representing a slight red shift in the SP band (462.4 nm to 487 nm) of AgNS-3 (prepared using PVP) on changing the surrounding media (water to DMSO). The red shift and broadening in the absorption band reflects the large size distribution of PVP coated AgNS. Moreover, there is no new band related to aggregation (at longer wavelength) has been observed as coating of PVP protects the NS from aggregation.

(iv) Electrokinetic studies of Ag nanospheres in different solvents

Electrokinetic behaviour (zeta potential and conductance) of particles is an important parameter to determine the stability of colloidal solution and arises due to the development of effective surface potential between the surface of nanoparticles and surrounding medium. The surrounding liquid layer of the particle exists in two parts; an inner region, where the counter ions are tightly bound to the particles, called as Stern layer and an outer, diffuse region of less firmly attached mobile ions. The potential difference which arises between the strongly bound stern layer and electroneutral region of the solution is called as Zeta potential (ζ) [59, 60]. The ζ is measured by electrophoresis technique in which the charged particle move under the influence of an applied electric field with respect to the liquid in which it is suspended. Variation in the zeta potential values (with the change of different solvents) determines the attraction or repulsion between the AgNS and the surrounding solvents. If all the particles in a colloid have a large negative or positive zeta potential then they will tend to repel each other and there will be very less chances of the particles to come closer.

Table.1 shows the variation in the zeta potential and conductance values of AgNS-2, AgNS-3 and AgNS-6 (ca. 4.7×10^{16} atoms), dispersed in 1.5 ml polar (water, ethanol, and DMSO) and non-polar solvent (heptane) as a function of their dipole moment. The measured zeta potential value ca. -5.59 mV for AgNS-2 has been found to increase to -

12.08 mV and -24.61 mV for AgNS-3 (PVP coated NS) and AgNS-6 (silica coated NS) in their aqueous dispersion media, respectively.

Table. 2 Variation in the zeta potential and conductance values of different AgNS on the addition of various solvents.

Sample code	Water (1.85 D)		Ethanol (1.68 D)		DMSO (3.96 D)		Heptane (0 D)	
	Zeta potential (mV)	Conductance (µS)	Zeta potential (mV)	Conductance (µS)	Zeta potential (mV)	Conductance (µS)	Zeta potential (mV)	Conductance (µS)
AgNS-2	-5.59	86	-10.42	75	-21.09	97	-6.97	73
AgNS-3	-12.08	54	-4.55	29	-18.04	14	-	-
AgNS-6	-24.61	1927	-19.10	404	-20.34	381	-	-

It is interesting to note here that AgNS-6 exhibits highest negative ζ value ca. -24.61 mV owing to dominant interparticle repulsion because of the presence of similarly charged ionic species (OH^- ions, present on the surface of AgNS-6 as well as in water). Moreover, AgNS-2 in DMSO exhibits high ζ value ca. -21.09 mV as compared to its aqueous suspension (-5.59 mV) due to the better charge separation as DMSO itself carry charge on its surface (Scheme.1). Moreover, AgNS (AgNS-2, AgNS-3 and AgNS-6) in DMSO dispersion resulted in almost comparable values (-21.09 mV, -18.04 mV and -20.34 mV) that confirmed their stability on changing the surrounding medium.

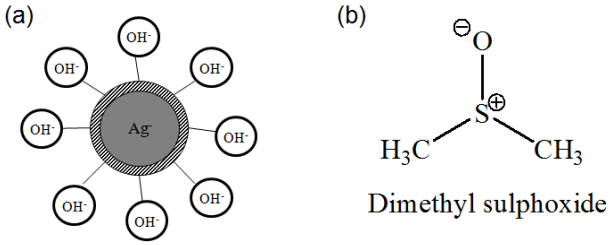

Scheme. 1 Representation of charge separation in AgNS (a) coated with silica and (b) dispersed in DMSO.

The observed ζ value for AgNS-2 in non-polar dispersion (heptane, ζ = -5.59 mV) is almost comparable to water suspension (-6.97 mV) because heptane being non-polar (0 D) does not carry any charge and hence, there is no influence of electric potential difference on the AgNS particle surface. In order to confirm this fact of electronic charge on the surface of AgNS particle, conductance of AgNS suspension in various solvents is

measured. The conductance of solution is dependent upon the concentration and mobility of the charged ions/species present in solution. The conductance 1927 µS of AgNS-6 in water is found to be highest owing to the free movement of the ions (OH^-) present on the silica surface (scheme 1). However, neutralisation of the charge/ ionic species dropped off the conductance to 381 µS on introducing the AgNS-6 in DMSO (as shown in scheme 1).

(v) Catalytic activity

Various AgNS catalysts have been used for the selective reduction of PNP (0.09 mM) by $NaBH_4$ (0.42 M) to corresponding amino derivates (*p*-aminophenol). Reduction of PNP to PAP causes a change in color (yellow to colorless) which is easily observed and reaction is well defined as no by-product is formed.

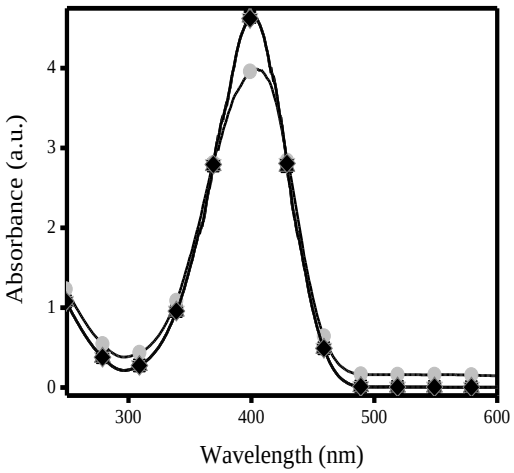

Figure. 7 Absorption spectra showing the PNP reduction only by $NaBH_4$ (reducing agent) without AgNS over a time course of 120 min.

Figure. 7 displayed absorption spectra for the reduction of PNP to PAP alone by $NaBH_4$ (without AgNS) and a negligible change has been observed over the time period of 120 min. It has been reported that during the reduction process, BH_4^- ions, being nucleophile donate electrons to metal NP and nitro compound act as electrophile capture electrons from metal NP. So, it is well established that BH_4^- ions and nitro compounds are simultaneously adsorbed on the surface of catalyst (AgNS) [61], when they were present together. Therefore, the presence of AgNS catalyst is very essential for the reduction reaction to be carried out.

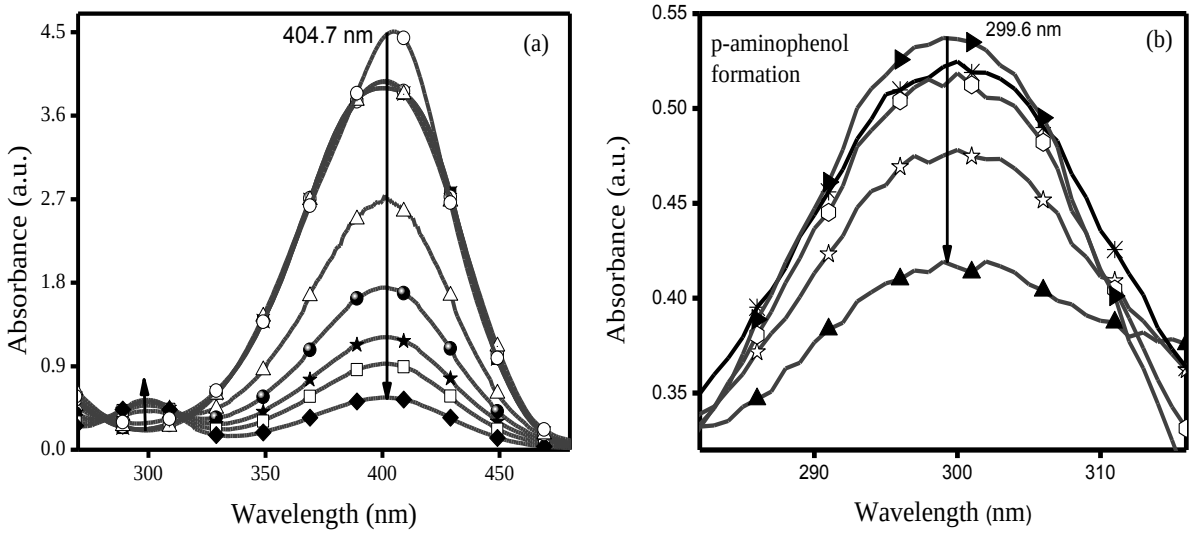

Figure. 8 (a) Changes in absorption spectra of PNP (0.09 mM) and the formation of PAP by AgNS-2 and (b) Enlarged view of absorption band between 280 to 315 nm shows the formation of PAP.

Figure 8a shows the typical UV-Vis absorption spectra of PNP (0.09 mM) reduced by $NaBH_4$ (0.42M) with the AgNS-2 (size = 13.5 nm, ca = 5.4×10^{18} atoms) as a catalyst. The strong absorption peak at 400 nm is the optical feature of PNP. The gradual decreasing of the peak intensity indicates the successive reduction of PNP and the two isosbestic points visible at 282 and 315 nm shows complete conversion of PNP to PAP. Meanwhile, the small absorption peak at 300 nm slowly increases with the reaction time, suggesting the formation of PAP. After 42 min., ~90% of PNP was reduced with the formation of PAP as shown in Figure 8b that showing magnified view (280 nm to 315 nm) of absorption band of PAP formation, which clearly indicates that initially there is no peak for PAP, but with the progress of PNP reduction, the amount of PAP starts to increase and the PNP reduction completed with reaction time (36 min). These results proved that the presence of AgNS is vital for complete reduction of PNP and only $NaBH_4$ addition will not serve the reaction.

(a) Effect of different sizes of Ag nanospheres on catalytic activity

Furthermore, by using the same number of the AgNS (ca = 5.4×10^{18} atoms) of different sizes (AgNS-1, AgNS-2, AgNS-3, AgNS-4, AgNS-5) as the catalyst, the conversion of PNP to PAP has been investigated as a function of reaction time as shown in fig. 9. The increment in the rate of disappearance of PNP (fig.9a) with the increase in the appearance of PAP (fig. 9b) on decreasing the size of AgNS (from 80 – 10 nm) has been noted.

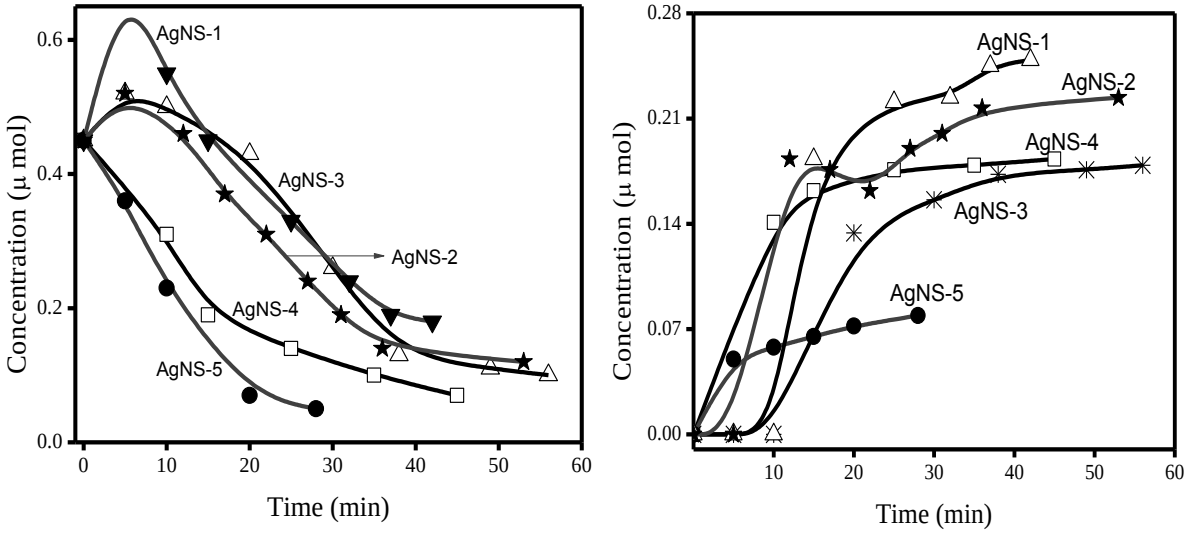

Figure. 9 Effect of adding different sizes of AgNS (AgNS-1, AgNS-2, AgNS-3, AgNS-4, AgNS-5, ca. 5.4×10^{18} atoms) on the (a) reduction rate of PNP and (b) production of PAP as a function of time.

The results indicated that the AgNS-1 showed highest percentage yield for the formation of PAP (55.3%) than that of AgNS-2 (49.7%), AgNS-3 (39.7%), AgNS-4 (40.6 %) and AgNS-5 (17.5 %) as seen from the fig 9b. Thus, the improved catalytic activity of AgNS-1 can be attributed to its smallest size (≈13.5 nm) as compared with other catalysts (AgNS-2, size ≈ 22 nm, AgNS-3, size ≈ 41.6 nm AgNS-4, size ≈ 50 nm, AgNS-5, size ≈ 80 nm) of larger sizes. AgNS-1 catalyst, being smallest in size have highest surface to volume ratio, more exposed surface electrons and therefore results in the better electron transport from the metal to substrate. It has also been observed that on coating of the NS with PVP (AgNS-3, AgNS-4 and AgNS-5) create some hindrance for transfer of electrons from the AgNS surface and resulted in the lower percentage yield (17.5%) of PAP production as compared to the non-coated particles (AgNS-1, 55.3%, and AgNS-2, 49.7%).

(b) Effect of concentration of Ag nanospheres on the PNP reduction

The rate of reduction for PNP was further examined by varying amount of AgNS-2 (5 - 20 μl, corresponds to ca. 2.73×10^{18} atoms - 10.92×10^{18} atoms of Ag) as a function of time as shown in fig. 10. It has been observed that the reduction of PNP and formation of PAP by varying amount of AgNS-2 (5 - 20 μl) was found to be remained almost constant, ca. 0.30 μmol, while the time taken for the completion of the reduction process was varied (36 – 120 min).

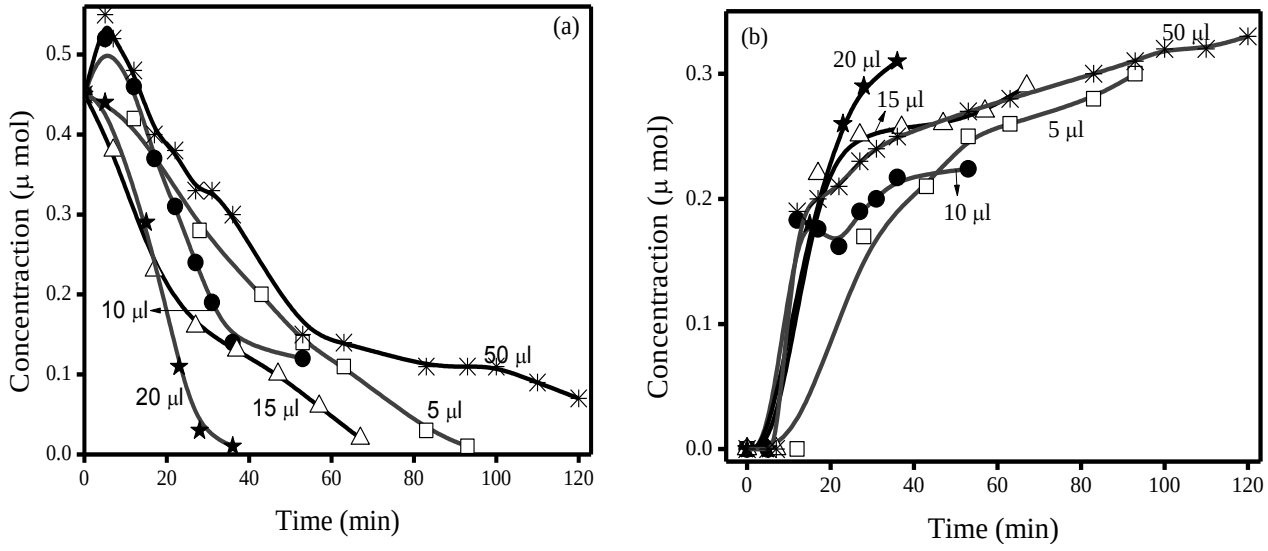

Figure. 10 Effect of varying the concentration of AgNS-2 (5 – 50 μl) on the (a) reduction rate of PNP and (b) production rate of PAP as a function of time.

The addition of 20 μl (10.92×10^{18} atoms) of AgNS-2 reduces the PAP within 36 min in comparison to the addition of 5 μl AgNS (2.73×10^{18} atoms) that takes 93 min for the

complete reduction. It is clearly depicted from the graph that on increasing the amount of AgNS upto a certain concentration (20 μl = 10.92×10^{18} atoms), reaction completes within 36 min, but on further increasing the amount of AgNS (50 μl = 27.31×10^{18} atoms), reduction took a longer time (120 min). It was assumed that the increasing dosage (50 μl) of the catalyst causes interruption for the efficient transfer of electrons to the reacting substrate and hence the reduction proceeds at a slower rate.Therefore, optimum amount of AgNS (10.92×10^{18} atoms) was needed to complete the PNP reduction within a short time.

(c) Catalytic activity by silica coated Ag nanospheres

To examine the efficiency of AgNS-6 as compared to bare AgNS-1, catalytic reduction of PNP was carried out as shown in figure 11. Fig 11a shows the absorption spectra of PNP

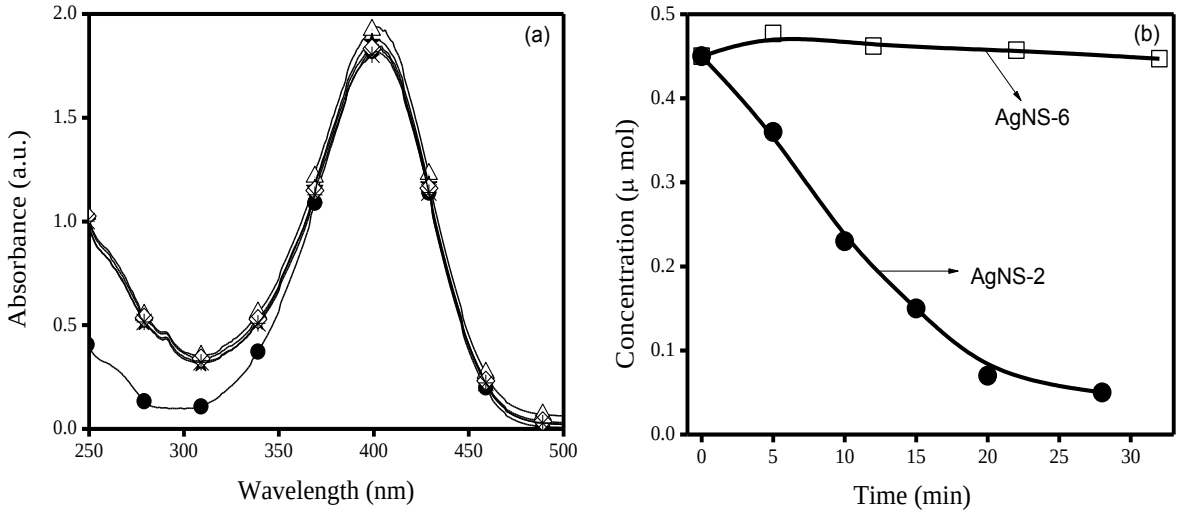

Figure. 11 (a) Changes in the absorption spectra of PNP (0.09 mM) in presence of SiO_2 coated AgNS (b) Comparative rate of catalytic reduction of PNP by AgNS-6 and AgNS-2.

(0.09 mM) reduced by $NaBH_4$ (0.42M) and SiO_2/AgNS (ca= 5.4×10^{18} atoms) as a catalyst. There is no change in the absorption peak (λ_{max} = 400 nm) of the PNP has been noticed even on keeping the reaction mixture (PNP, $NaBH_4$, and AgNS-6) for 180 min.

In comparison to bare AgNS, SiO_2/AgNS displayed negligible catalytic reduction of PNP that was ascribed to its thicker shell thickness (fig.11b). In case of AgNS, there is a direct contact of AgNS surface with target PNP molecules. Hence, the ease of electron relay from AgNS to substrate makes it superior than SiO_2 shell bound on AgNS. However, by controlling the SiO_2 layer thickness, stable and optimum catalytic efficiency of may achieve.

7. Conclusion

The results obtained in the present work are summarized in Table.2.

Table. 2. Comparative size, optical, electrokinetic and catalytic properties of prepared Ag-Nanospheres.

Sample Code	Observed SPR Band (nm)	TEM Size (nm)		Zeta Potential value* (mV)	PNP Reduced (µmol)	PAP Formed (µmol)	Percentage Yield (%)
		Reported (ref)	Obtained From TEM and DLS				
AgNS-1	392.7	10-15 [24]	≈ 13.5	-	0.27 (0.18)**	0.249	55.3
AgNS-2	419.6	> 18 [27]	≈ 22	-5.59	0.33 (0.12)**	0.224	49.7
AgNS-3	462.4	> 40 [28]	≈ 41.6	-	0.35 (0.10)**	0.179	39.7
AgNS-4	474.6	> 45 [29]	≈ 50	-12.08	0.38 (0.07)**	0.183	40.6
AgNS-5	522.5	> 75 [28]	≈ 80	-	0.40 (0.05)**	0.079	17.5
AgNS-6	409.9	-	-	-24.61	0.01 (0.44)	0.00	-

*Measured in water **remaining amount of PNP

In summary, AgNS of different sizes (10 - 80 nm) has been synthesized, characterized and compared their various physico-chemical, optical, electrokinetic and catalytic properties. Furthermore, PVP and silica was used as protective agents to increase the stability of AgNS by preventing their oxidation. Stability of the AgNS was examined through zeta potential/conductance measurements in various polar and non-polar solvents and was concluded that the silica coated nanospheres shows the highest stability with -24.61 mV over the uncoated AgNS particles (-5.59 mV).

To evaluate the catalytic performance of as fabricated AgNS of different sizes, *p*-nitrophenol was chosen as organic model compound. Reduction process proceeds at a higher rate with decreasing the size of AgNS. Silica coated silver nanospheres shows negligible activity towards the reduction of *p*-nitrophenol but on the other side, bare AgNS (uncoated NS) hasten the reduction rate (49.7 %) due to ease of electron transfer for reduction process.

Besides this, PVP coated AgNS of sizes (≈ 41.6 nm, ≈ 50 nm and ≈ 80 nm) seems to be recessive (AgNS-5, 17.5 %) over without PVP coated particles (AgNS-1, 55.3 %)

ascribed to their hindrance in participation in reduction. The optimization in thickness of silica shell still needs to study for better response in the optoelectronic and catalysis field.

8. References

1. Rao, Y.; Antonelli, D. M., *J. Mater. Chem*. **2009**, 19, 1937.
2. Sun, R. W. Y.; Ma, D. L.; Wong, E. L. M.; Chi-Ming Che, C. M., *Dalton Trans.*, **2007**, 4884.
3. K. Kalyanasundaram, K.; Gratzel, M., *Coord. Chem. Re*v. **1998,** 177, 347.
4. Choi, H.; Chen, W. T.; Kamat, P. V., *ACS nano.* (in press).
5. Hayton, T. W.; Legzdins, P.; Sharp, W. B., *Chem. Rev.* **2002,** 102, 935.
6. Ye, F.; Ma, X.; Xiao, Q.; Li, H.; Zhang, Y.; Wang, J., *J. Am. Chem. Soc.* **2012**, 134, 5742.
7. Corma, A.; Perez, A. L.; Sabater, M. J., *Chem. Rev.* **2011**, 111, 1657.
8. Castillo, V. A.; Kuhn, J. N., *J. Phys. Chem. C*, **2012** (in press)
9. Vyas, R.; Gao, G.-Y.; Harden, J. D.; Zhang, X. P., *Org. Lett.* **2004**, 6, 1907.
10. Piber, M.; Jensen, A. E.; Rottlander, M.; Knochel, P., *Org. Lett.* **1999**, 1, 1323.
11. Srimani, D.; Bej, A; Sarkar, A., *J. Org. Chem.* **2010,** 75, 4296.
12. EL- Sayed, M. A., *Acc. Chem. Res.* **2001**, 34, 257.
13. Haruta, M., *Catal. Today*, **1997**, 36, 53.
14. Eustis, S.; El-sayed, M. A. *Chem. Soc. Rev*. **2006**, 35, 209.
15. Ghosh, S. K.; Pal, T.; Kundu, S.; Nath, S.; Pal, T. *Chem. Phys. Lett.* **2004**, 395, 366.
16. Kamat, P. V., *J. Phys. Chem. B*, **2002,** 106, 7729.
17. Sajanlal, P. R.; Sreeprasad, T. S.; Samal, A. K.; Pradeep, T., *Nano Rev.* **2011**, 2, 5883.
18. Ghosh, S. K.; Pal, T., *Chem. Rev*. **2007,** 107, 4797.
19. Ghosh, S. K.; Kundu, S.; Mandal, M.; Pal, T. *Langmuir*, **2002**, 18, 8756.
20. Zeng, J.; Zhang, Q.; Chen, J.; Xia, Y., *Nano Lett.* **2010**, 10, 30.
21. Haruta, M., *Gold Bull.* **2004**, 37, 27.
22. Haruta, M., *J. New. Mat. Electrochem. Syst.* **2004**, 7, 163.
23. Haruta, M., *Chem. Rec.* **2003**, 3, 75.
24. Haruta, M., *J. New. Mat. Electrochem. Systems,* **2004**, 7, 163.
25. Mulvaney, P., *Langmuir* **1996,** *12, 788.*
26. Liz-Marzan, L. M., *Langmuir,* **2006,** 22, 32.
27. Lisiecki, I., *J. Phys. Chem. B*, **2005**, 109, 12231.

28. Wong, K. K. Y.; Liu, X., *Med. Chem. Commu*. **2010**, 1, 125.
29. Daniel, M. C.; Astruc, D., *Chem. Rev.* **2004,** 104, 293.
30. Veith, G. M.; Lupini, A. R.; Rashkeev, S.; Pennycook, S.; Mullins, D. R.; Schwartz, V.; Bridges, C. A.; Dudney, N. J., *J. Catal.* **2009**, 262, 92.
31. Tiwari D. K.; Behari, J.; Sen, P., *World Appl. Sci J.* **2008**, 3, 417.
32. Martinez- Castanon, G. A.; Nino-Martinez, N.; Martinez-Gutierrez, F.; Martinez-Mendoza, J. R.; Ruiz, F., *J. Nanopart. Res.* **2008**, 10, 1343.
33. Ray, P. C., *Chem. Rev.* **2010,** 110, 5332.
34. Bennette, C. J.; Swanson, L. W.; Charbonnier, F. M., *J. Appl. Phys.* **1967**, 28, 634.
35. Xu, R.; Wang, D.; Zhang, J.; Li, Y., *Chem. Asian J.* **2006**, 1, 888.
36. Huang, T.; Meng, F.; Qi, L., *J. Phys. Chem. C*, **2009**, 113, 13636.
37. Tzhayik, O.; Sawant, P.; Efrima, S.; Kovalev, E.; Klug, J. T., *Langmuir*, **2002,** 18, 3364.
38. Pastoriza-Santos, I.; Pe´rez-Juste, J.; Liz-Marzan, L. M., *Chem. Mater*. **2006,** 18, 2465.
39. EL Badawy, A. M.; Luxton, T. P.; Silva, R. G.; Scheckel, K. G.; Suidan, M. T.; Tolaymat, T. M., *Environ. Sci. Techno.* **2010,** 44, 1260.
40. Mcnamee, C. E.; Matsumoto, M.; Hartley, P. G.; Mulvaney, P.; Tsujii, Y.; Nakahara, M., *Langmuir*, **2001,** 17, 6220.
41. Liao, J.; Zhang, Y.; Yu, W.; Xu, L.; Ge, C.; Liu, J.; Gu, N., *Colloids Surf. A: Physicochem. Eng. Aspects*, **2003**, 223, 177.
42. Xia Guo, X.; Zhang, Q.; Sun, Y.; Zhao, Q.; Yang, J., *ACS Nano.* **2012**, 6, 1165.
43. Filippo, E.; Manno, D.; Buccolieri, A.; Giulio, M. D.; Serra, A., *Superlattices microstruct.* **2010**, 47, 66.
44. Nam, S.; Parikh, D.V.; Condon, B.D.; Zhao, Q.; Tarver, M. Y., *J. Nanopart Res*., **2011**, 13, 3755.
45. Bogle, K.A.; Dhole, S.D.; Bhoraskar, V.N. *Nanotechnology*, **2006**, 17, 3204.
46. Sarkar, A.; Kapoor, S.; Mukherjee, T., *Res. Chem. Intermed*. **2010**, 36, 411.
47. Patel, K.; kzpoor, S.; Dave, D. P.; Mukherjee, T., *J. Chem. Sci.* **2005**,117, 53.
48. Santos, I. P.; Marza, L. M., *Langmuir,* **2002,** *18*, 2888.
49. Kobayashi, Y.; Katakami, H.; Mine, E.; Nagao, D.; Konno, M.; Liz-Marzan, L. M., *J. Colloid Interface Sci.* **2005**, 283, 392.
50. Jie Zeng, J.; Qiang Zhang, Q.; Jingyi Chen, J.; Xia, Y., *Nano Lett.* **2010**, 10, 30.

51. Chirea, M.; Freitas, A.; Freitas, B. S.; Ghitulica, C.; Pereira, C. M.; Silva, F., *Langmuir*, **2011**, 27, 3906.
52. Kim, J. S.; Kuk, E.; Yu, K. N.; Kim, J. H.; Park, S. J.; Lee, H. J.; Kim, S. H.; park, Y. K.; Park, Y. H.; Hwang, C. Y.; Kim, Y. K.; Lee, Y. S.; Jeong, D. H.; Cho, M. H., *Nanomedicine: Nanotechnology, Biology, and Medicine*, **2007**, 3, 95.
53. Hirakawa, T.; Kamat, P. V., *J. Am. Chem, Soc.* **2005**, 127, 3928.
54. Tada, H.; Ishida, T.; Takao, A.; Ito, S.; Mukhopadhyay S.; Akita, T.; Tanaka, K.; Kobayashi, H., *Chem. Phys. Chem.* **2005**, 6, 1537.
55. Ratyakshi; Chauhan, R. P., *Asian J. Chem.* **2009**, 21, 113.
56. Silvert, P. Y.; Herrera-Urbinab, R.; Tekaia-Elhsissena, K., *J. Mater. Chem.* **1997**, 7, 293.
57. Yang, Y.; Matsubara, S.; Xiong, L.; Hayakawa, T.; Nogami, M., *J. Phys. Chem. C,* **2007,** 111, 9095.
58. Cobley, C. M.; Skrabalak, S. E.; Campbell, D. J.; Xia, Y., *Plasmonics*, **2009**, 4, 171.
59. Mukherjee, B.; Weaver, J. W., *Environ. Sci. Technol.* **2010,** 44, 3332.
60. Kim, T.; Lee, K.; Gong, M.; Joo, S. W., *Langmuir,* **2005,** 21, 9524.
61. Wunder, S.; Polzer, F.; Lu, Y.; Mei, Y.; Ballauff, M., *J. Phys. Chem. C,* **2010,** 114, 8814.